

Modelling of fluid motion in spacecraft propellant tanks - Sloshing

N. Fries*[©], P. Behruzi*, T. Arndt*, M. Winter*, G. Netter*, U. Renner*

*Astrium Space Transportation, Bremen, Germany

[©]Nicolas.Fries@astrium.eads.net

Abstract

Gas-free liquid expulsion is a key function of propellant tanks in spacecraft. It is essential to accurately predict the fluid motion in both, an accelerated environment as well as μg conditions. Propellant sloshing in tanks also influences the rigid body motion of the spacecraft, which then needs to be controlled by the reaction control system. Therefore, it is necessary to pay special attention to the sloshing issue, which includes e.g. the sloshing forces and torques imposed by the liquid motion in the tank, and as a result the corresponding shifts of the CoG. Various fluid mechanical approaches exist to determine the sloshing behaviour including:

1. Spring-mass or pendulum models are frequently used to evaluate sloshing forces and torques of the rigid body. They are frequently applied for sloshing in an accelerated environment, e.g. during the ascent phase and in-orbit manoeuvres. For simple geometries the parameters of the spring-mass or pendulum model can be derived from literature. However, for real tank geometries a number of Astrium ST in-house tools exist which are used to generate the models representing the propellant behaviour.
2. CFD tools such as FLOW-3D may be used to predict the sloshing behaviour. Clearly these tools are often applied in a low-g environment where spring-mass or pendulum models are not valid any more, especially when sloshing occurs in capillary dominated regimes.
3. For μg applications also closed loop CFD simulation tools are used to consider the coupling between sloshing motion, rigid body motion and the reaction control system.

Details concerning the theoretical background as well as aspects concerning their verification e.g. by tests will be given. Also an overview of the various tools applied at Astrium ST and the actual research programs will be presented.

1. INTRODUCTION - SLOSHING MODES

In this section the existing sloshing modes are briefly introduced including damping and common sloshing models. Since spaceflight propulsion is often based on liquid propellants it was soon realised that the behaviour of the liquid in the spacecraft tanks is of major interest regarding the flight dynamics. This has triggered a lot of fundamental research in the early 1960 when NASA started their Gemini and Apollo programs, e.g. by Abramson et al. [10][11][11].

When liquids slosh in a closed container there are multiple configurations (modes) in which the surface may evolve. Commonly, the different modes can be defined by their wave number m (number of waves in circum-

ferential direction) and by their mode number n (number of waves in radial direction) as shown in Figure 1.

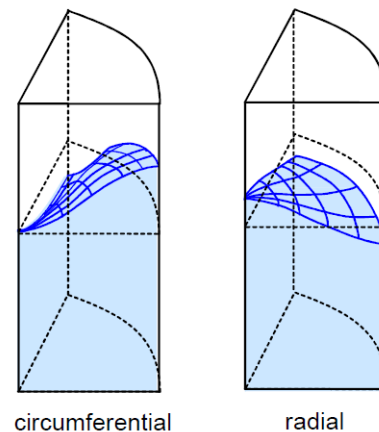


Figure 1: Slosh modes for a radial tank (figure taken from [2]).

E.g. $n = 1$ refers to the first sloshing mode, $n = 2$ to the second mode and so on. Details on the different sloshing modes shall be provided in the following.

In general, it exist two types of sloshing modes: the symmetrical and the asymmetrical types. The first asymmetrical modes - most commonly occurring in spacecraft tanks - are introduced in Figure 2.

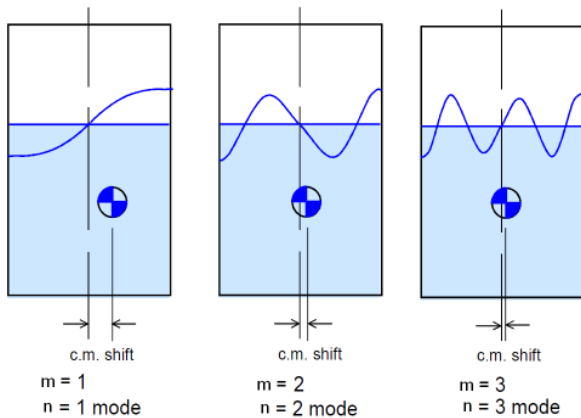


Figure 2: Slosh wave shapes for the first three asymmetrical modes of a rectangular tank (figures are slightly modified taken from [2]).

As shown in Figure 2, the CoG shifts when the liquid moves to provoke forces and torques acting on the tank shell. For the first mode the CoG shift is much larger than for the other modes. Therefore - to describe the dominant fluid motions in a tank - often only the first mode representing the most critical case is considered. The higher the sloshing mode, the higher is the corresponding natural frequency. Details on the natural frequency are provided later.

In Figure 3, the symmetrical modes are shown. The frequencies for the symmetrical modes are always higher than for the corresponding asymmetrical modes. For the symmetrical modes, the occurring lateral forces and torques can be neglected as there is also no CoG shift. Therefore they are of less significance regarding the propellant behaviour in spacecrafts and satellites.

Besides the above mentioned sloshing modes there also exists a swirling mode. This mode

typically occurs when the liquid is laterally excited with a frequency close to its first natural frequency (see Figure 6). The direction of the rotational motion is random and may spontaneously change.

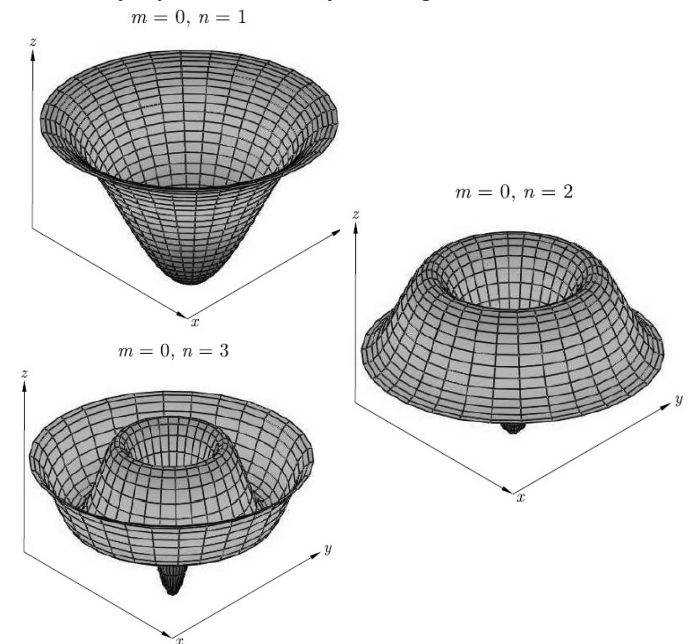


Figure 3: Slosh wave shapes for the first three symmetrical modes in a cylindrical tank. No lateral CoG shift occurs.

2. INTRODUCTION - DAMPING

Due to viscous effects (friction) the amplitude of the sloshing wave decreases over time when the external excitation is stopped. This is called damping. For a given tank and liquid, the damping behaviour can be predicted by analytical models which have been validated by experimental test, e.g. see [2][12]. Most commonly, for real tanks with internal equipment such as reservoirs, vanes or baffles, the damping characteristics are increased with respect to the bare tank configuration.

Please note that the following damping models are valid for linear systems only (e.g. up to about 15° deflection angle).

The damping behaviour of the force or wave amplitude decay after stopping the excitation is represented by the logarithmic decrement

$$\Lambda = \frac{1}{i} \ln \frac{A_0}{A_i} \quad (1)$$

where A_0 is the initial wave amplitude [m] or the wave force [N] for harmonic oscillations, A_i is the i^{th} amplitude and i is the number of cycles. The damping ratio γ , also denoted D , in [-] is determined from the logarithmic decrement by

$$\gamma = \frac{\Lambda}{\sqrt{4\pi^2 - \Lambda^2}} = \frac{|dE/dt|}{2\omega E} \quad (2)$$

In this equation, γ can also be regarded as the amount of mechanical energy lost by viscous friction (transferred into heat) over one cycle of sloshing in relation to the total mechanical energy E [2].

The damping of the sloshing motion strongly depends on viscous effects, and therefore on the viscosity of the sloshing liquid. The other main parameters which need to be considered are e.g. the fill level, the shape of the tank shell and the interior components. It has been found that a useful scaling parameter is the non-dimensional (modified) Reynolds number or the Galilei number that are defined as

$$Re_1 = \frac{\nu}{\sqrt{aL^3}} = \frac{1}{\sqrt{Ga}} \quad (3)$$

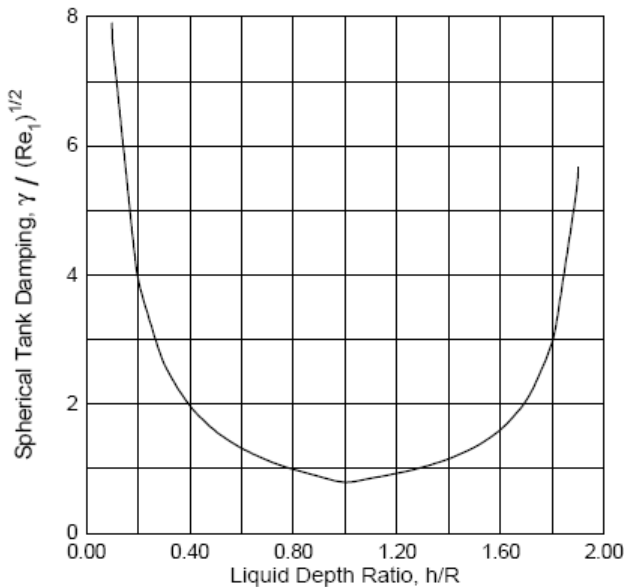


Figure 4: Damping for a spherical tank. $h/R=1$ corresponds to a fill level=50% (extracted from [2]). Minimum damping value at 50% fill level (cylindrical part of the tank).

with $Ga = aL^3/\nu^2$, where ν is the fluid kinematic viscosity, and L is the characteristic length scale, e.g. the tank radius (see [2] for further details).

As an example Figure 4 displays the damping ratio (scaled with Re_1) plotted over the tank fill level for a spherical tank. It can be observed that the minimum damping occurs for 50 % tank fill level, while for larger or smaller fill levels the damping ratio significantly increases.

It is also possible to analytically determine the impact of anti sloshing devices, such as vertical baffles, ring baffles or bladders / diaphragms. The following approximation to estimate the damping might be useful: For very highly damped tanks (e.g. applying several anti sloshing baffles) damping ratios of about 0.05 may be reached [2], for "standard" tank shapes the value may be in the order of magnitude smaller 0.005, or even lower (e.g. for spherical tanks).

3. INTRODUCTION - SLOSHING MODELS

For various applications it is sufficient to apply a simplified model that describes the sloshing behaviour of a liquid in an excited tank. The advantage of these models include that they characterize sloshing with sufficient accuracy, but they only consist of simplified equations. This is in contrast to the more complex determination of the sloshing behaviour using e.g. CFD, analytical expressions or other software tools. Therefore it is common to use the more complex tools to generate a specific sloshing model (e.g. for a propellant tank) while the generated sloshing model is used as an input to GNC calculations (Monte Carlo etc.).

Most commonly, two frequently used types of sloshing models are applied. The first one is the pendulum model, the second one the spring-mass model. Both model types are based on the approach to transform the liquid motion in the tank to the motion of a mass attached to a pendulum or a mass attached to a spring, respectively. For these systems

(pendulum and spring-mass) simplified equations exist, but the determination of the corresponding parameters is however more complex. These can be either determined by analytical models (for simple geometries), or by numerical tools e.g. as described in chapters 4, 5 and 6.

3.1. Pendulum model

For the pendulum model (see Figure 5), the natural frequency is defined as

$$\omega = \sqrt{\frac{a}{l_n}} \quad (4)$$

where a is the acceleration acting on the system (e.g. $1g$ for a pendulum on earth) and l_n is the pendulum length. Please note that the index "n" denotes the sloshing mode. Obviously when a is varied, the natural frequency of the pendulum changes. This is a useful feature of the pendulum model for spacecraft and satellite applications where a is typically variable. In terms of excitation, the motion of the pendulum as a function of time is given by

$$\varphi(t) = \varphi_{\max} \sin(\omega t) \quad (5)$$

where φ is the angle of inclination of the pendulum compared to its static position, φ_{\max} is the initial maximum angle of the pendulum (depending on its excitation), and t is the time scale. Please note that above equation represents an approximation and is usable up to about $\varphi_{\max} = 15^\circ$ (~0.5 % error on natural frequency).

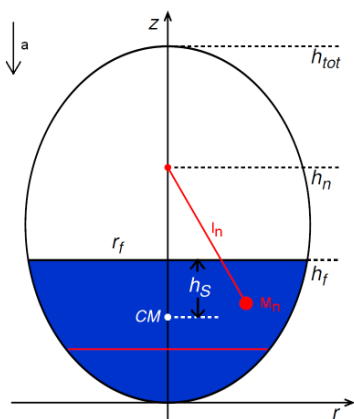


Figure 5: Pendulum model.

The total mass of the liquid in the tank is split into a static mass m_0 (liquid bulk) that is not affected by the sloshing motion and the sloshing pendulum masses $m_1; m_2; \dots$ of the different modes so that

$$m_{\text{liquid}} = m_0 + m_1 + m_2 + \dots \quad (6)$$

3.2. Spring-mass model

For the spring-mass model (see Figure 7), the sloshing mass is located at the same position as the sloshing mass for the pendulum model (not at the pendulum hinge height!). Thus, the natural frequency is defined as

$$\omega = \sqrt{\frac{c_n}{m_n}} \quad (7)$$

where c_n is the spring constant and m_n is the sloshing mass attached to the spring. For a spring-mass model the natural frequency does not change automatically when a is changed. Therefore, c_n needs to be adjusted for each acceleration level. The motion of the mass as a function of time is given by

$$x(t) = x_{\max} \sin(\omega t) \quad (8)$$

where x is the displacement of the mass compared to its static position, while x_{\max} is the initial maximum displacement of the mass (depending on its excitation).

3.3. Response curve

If the excitation corresponds to a harmonic oscillation, the differential equation of motion is given by

$$\ddot{x}(t) + 2\gamma\omega_{mn}\dot{x}(t) + \omega^2x(t) = x_A\omega_{mn}^2\cos(\omega t) \quad (9)$$

The steady state solution of this equation can be determined to be

$$x(t) = x_A B \cos(\omega t - \phi_s) \quad (10)$$

where ϕ_s is the phase shift, B the amplitude ratio (amplitude of system response divided by the excitation amplitude x_A) yielding

$$B = \frac{\eta^2}{\sqrt{(1-\eta^2)^2 + 4\gamma^2\eta^2}} \quad (11)$$

and η the frequency ratio (frequency of excitation divided by the natural frequency of system) so that

$$\eta = \frac{\omega}{\omega_{nn}} \quad (12)$$

The response curve is plotted in Figure 6 showing the different amplitude ratios as a function of frequency ratio and damping ratio. While the excitation frequency comes close to the natural frequency the response is significantly increased (this regime should be avoided in applications). Additional damping reduces the response, but for typical tank damping ratios no significant relaxation can be expected (without considering baffles etc). Please note that this is only valid for "ideal" systems; for real tank geometries the response curve may differ and needs to be determined e.g. by test or by calculation.

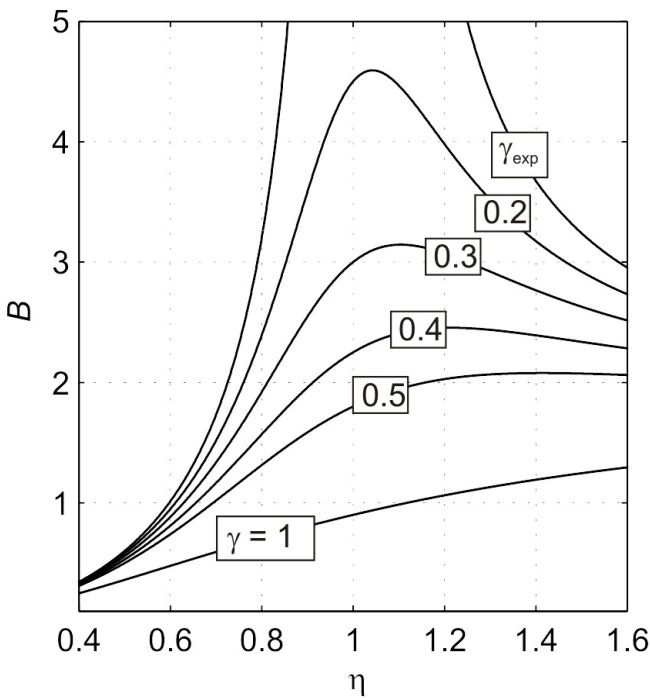


Figure 6: System response curve according to Eq. (11).

3.4. Resulting forces

The force imposed by the spring mass or pendulum system is equal to the force of the sloshing liquid. Thus, the lateral sloshing force gives

$$F_n(t) = c_n \cdot x(t) = a m_n \sin(\varphi(t)) \quad (13)$$

It has to be noted that if the whole tank is accelerated / laterally excited, the resulting force gives

$$F_{a_lat} = m_{\text{tank}} \cdot a_{lat} \quad (14)$$

which has to be added to the dynamic sloshing force defined in equation (13). Either way, the pendulum model and the spring-mass model can both be converted into the other form. This is shown schematically in Figure 8.

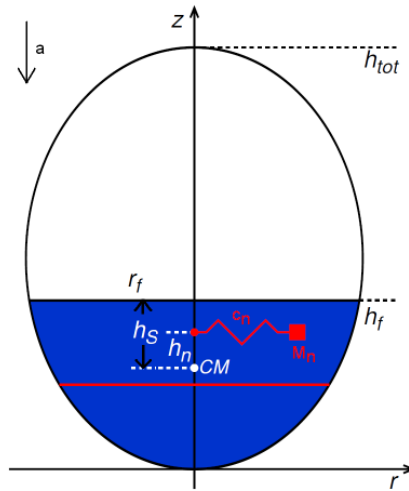
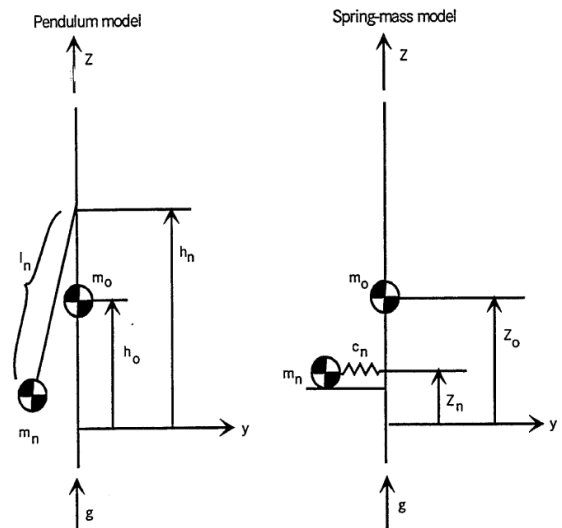


Figure 7: Spring mass model.



$$\frac{c_n}{m_n} = \frac{g}{l_n}$$

$$z_n = h_n - l_n \quad z_o = h_o$$

Figure 8: Equivalent mechanical models for lateral sloshing.

Please note that standard sloshing models mostly do not include non-linear effects of the fluid motion and therefore are typically only applicable up to about 15° deflection angle.

4. DESCRIPTION OF THE SMALLSLOSH TOOL (SMALL AMPLITUDES)

The program SMALLSLOSH [1] computes natural frequencies for linear sloshed liquids (e.g. sloshing mode $m = 1$; $n = 1$) in axisymmetric tanks and predicts equivalent mechanical models. The application is based on the potential theory where the liquid is considered to be inviscid and incompressible (details are provided in [2]). Thus, the velocity field can be described by the Laplace equation

$$\nabla^2 \Phi = 0 \quad (15)$$

where $\nabla \Phi = \vec{u}$, and Φ is the velocity potential of the liquid. Solving this equation with the corresponding boundary conditions at the tank bottom and walls one obtains the solutions of the liquid motion and the sloshing behaviour. For a cylindrical tank, the velocity potential is defined in cylindrical coordinates for the sloshing mode (m, n)

$$\Phi = \sum_m \sum_n A_{mn} \cosh\left(\varepsilon_{mn} \frac{z}{R}\right) J_m\left(\varepsilon_{mn} \frac{r}{R}\right) \dots \dots \cos(m\theta) e^{i\omega_{mn} t} \quad (16)$$

In this equation, A_{nm} is an arbitrary constant determined from the initial conditions and ε_{mn} gives the roots of the derivative of the Bessel function of the first order J_m .

The equations used in the applications are taken from literature such as [2][9][11]. Some modifications are considered based on [8]. Dialogs support the user in the program handling and the results are presented in graphical form as well as printed in data files for off-line evaluation as shown in Figure 9.

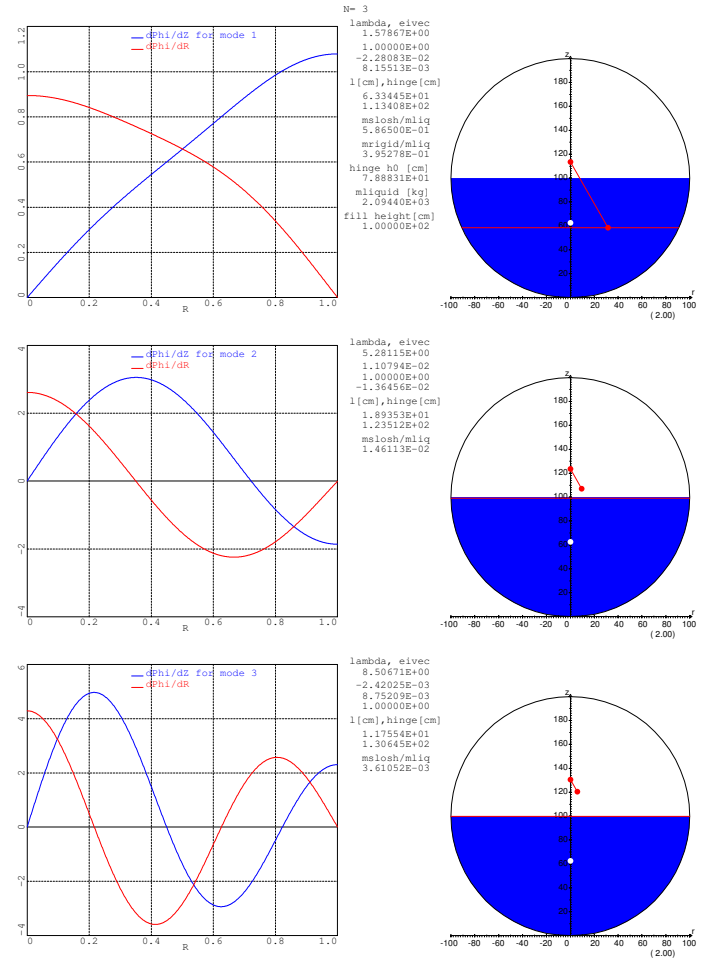


Figure 9: Result for three modes with the pendulum model.

5. DESCRIPTION OF THE LAMPS2 TOOL (LARGE AMPLITUDES)

The program LAMPS2 allows the computation of the bulk motion of a liquid stored in a cylindrical tank with two identical ellipsoidal domes as shown in Figure 10. The external accelerations of the tank inducing the liquid motion are constraint to the (Y-Z)-plane, i.e. the liquid centre of mass (CM) moves on a plane curve called the constraint line. This approach is based on [5]. Furthermore only parallel displacements of the tank are allowed. The initial position of the fluid CM is determined by the equilibrium position in a 1g gravity field depending on the inclination angle ϑ and the fill level of the tank. The parallel displacement refers to an aspect of the so called LAMPS2 in-house software.

This software computes the sloshing motion of the liquid centre of gravity (CoG), which is following the tank wall geometry. The CoG of the liquid is sloshing in one plane (Y-Z plane in this case). Parallel displacement means that the rotational axis does not need to be in the origin tank since the tool is able to evaluate sloshing in a rotating tank. A screenshot of the application showing a rigid sloshing motion is provided in Figure 11.

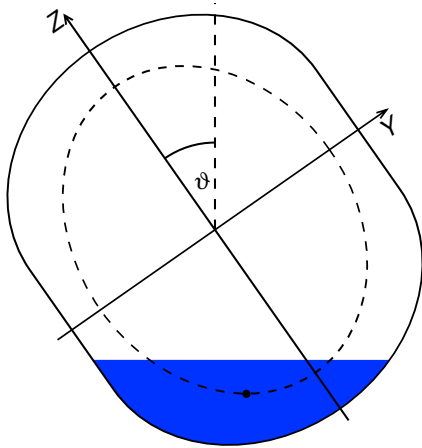


Figure 10: LAMPS2 program with sloshing liquid. The liquids CoG moves on a constraint line (dashed).

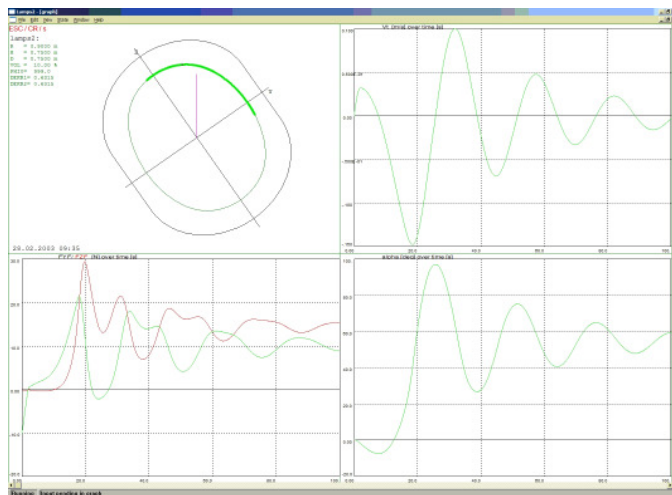


Figure 11: Screen shot of the LAMPS2 program.

6. DESCRIPTION OF CFD WITH FLOW-3D®

The standard tool for dynamic sloshing calculations used at Astrium ST is the CFD tool FLOW-3D by Flow Science Inc. [6]. This tool is used to predict linear and non-linear sloshing behaviour under high- g (e.g. ascent phase) and μg conditions (e.g. ballistic phase). The validation of the tool has been performed by Astrium ST within various internal R&D programs. Many benchmark experiments - e.g. in the drop tower ZARM in Bremen - were carried out for verification of the tool. The performed benchmark experiments clearly demonstrate the suitability and good accuracy of the software in terms of predicting the propellant motion in spacecraft and satellite tanks.

During orbital manoeuvres, e.g. satellites performing North/South station keeping manoeuvre, there is a reorientation of the propellant from the initial microgravity configuration towards a configuration often dominated by hydrostatic forces. After the orbit manoeuvre is finished, again, there is a reorientation of the propellant towards the microgravity configuration, where capillary forces dominate as shown in Figure 12.

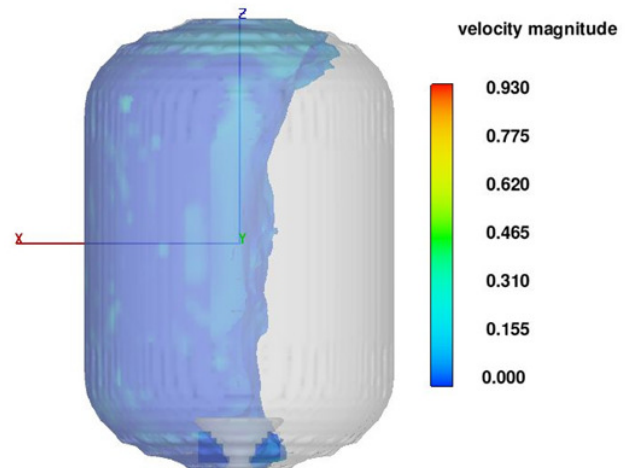


Figure 12: CFD simulation of transient propellant reorientation.

In order to model the sloshing motion during the horizontal transport a FLOW-3D® simulation was carried out, as depicted in

Figure 13 as example for the Proton launcher rail transport.

Pendulum models or spring-mass models (if applicable) from Flow-3D CFD results can be generated using the Astrium ST in house tool SLOSHFIT.



Figure 13: Modelling of propellant sloshing during horizontal transport of the partly filled tank.

7. DESCRIPTION OF FiPS TOOL (COUPLING ALGORITHM BETWEEN THE RIGID BODY MODEL AND THE FLOW-3D® MODEL)

The following chapter gives a brief introduction to the in-house FiPS tool used in Astrium ST [3][4]. FiPS (Final Phase Simulator) is a closed loop simulation tool, which was originally developed for the analysis of propellants in rocket upper stages. The FiPS tool manages the coupling between the liquid motion - mostly responsible for the disturbances during the ballistic phase - and the controller that must counteract the disturbances by according reaction control thruster firings. One of the advantages of the FiPS code is the possibility to realize the liquid motion by embedding enhanced CFD tank models that interact with the controller algorithm by exchanging simulated flight data (e.g. providing propellant force to the controller and receiving accelerations). At Astrium ST the coupling has been realized with the CFD software FLOW-3D® by Flow Science [6]. By using FiPS, it is possible to check and if necessary to filter the CFD output data ensuring that no numerical

disturbances influence the rigid body motion. A simplified schematic representation of the interaction between FiPS and FLOW-3D® is shown in Figure 14. Furthermore, an overall simulation environment structure is provided in Figure 15.

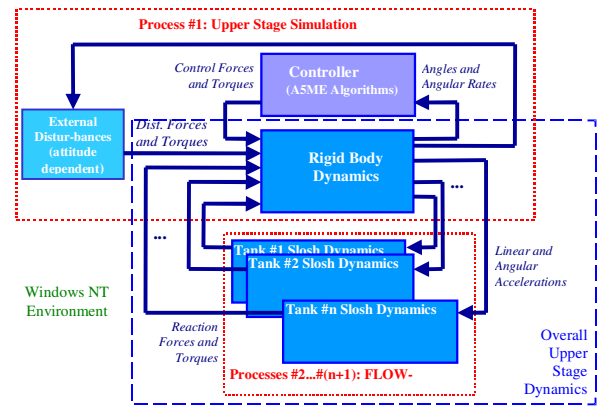


Figure 14: Simplified representation of the interaction between the rigid body model and the FLOW-3D® model through FiPS.

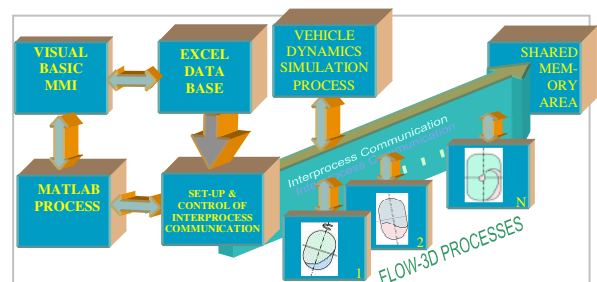


Figure 15: Overall Simulation Environment structure.

The rigid body model exchanges acceleration as well as forces and torques generated by propellant motion with the fluid dynamic model. Please note that the rigid body model may also include an active flight controller and the corresponding impulses from the reaction control propulsion system (implementation of according cold gas / hot gas thruster models). Furthermore, simplified models, such as spring-mass models, can be implemented in FiPS in the same manner as successfully realized with the FLOW-3D® models in the present case. Thus it is possible to compare the simplified models with the CFD computation by modifying the

pendulum parameter to adapt them in a more sophisticated way.

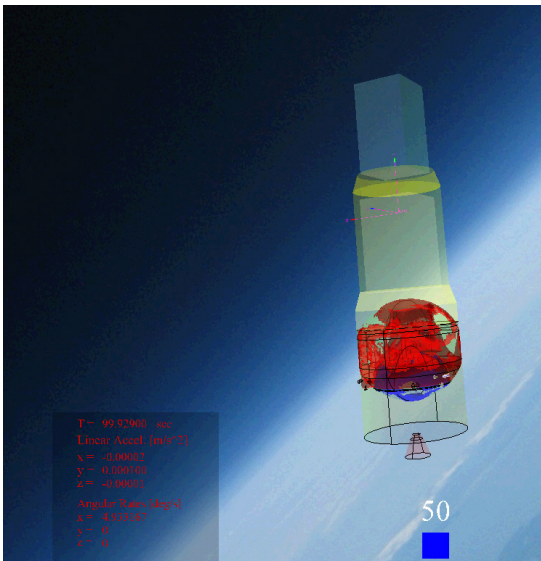


Figure 16: Propellant sloshing motion inside the LH2 tank (red) and the LOX tank (blue) in case of spin-up manoeuvre (here Ariane A5ME upper stage).

As an example Figure 16 shows the sloshing motion in case of a spin-up manoeuvre in a typical upper stage application. The illustration shows the tank configuration of the Ariane A5ME upper stage.

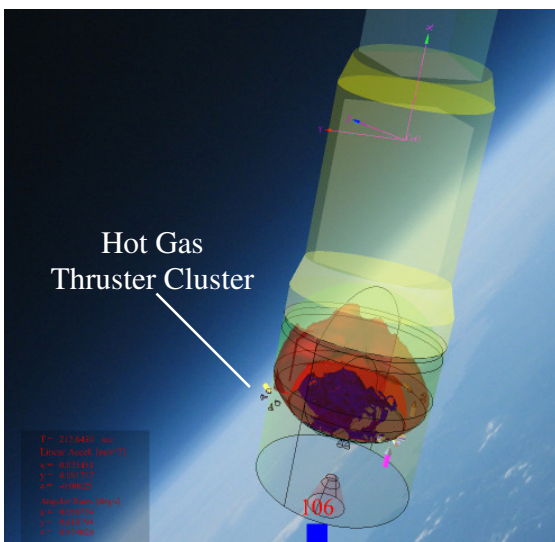


Figure 17: Propellant sloshing motion inside cryogenic upper stage tanks (here Ariane A5ME upper stage) and corresponding cold gas and hot gas thrust pulse during a re-orientation manoeuvre.

The illustration in Figure 16 shows the reorientation of the liquid towards the tank wall when the stage goes into a certain spin motion. As shown in Figure 16, the propellant motion in the tanks during transient manoeuvres can be very chaotic making it difficult to reproduce the propellant behaviour by simplified pendulum models. Thus, a visualization tool has been developed allowing the observation of the propellant motion inside the tanks including the motion of the stage and the thrust pulses, as shown in Figure 17.

8. SLOSHING OF CRYOGENIC LIQUIDS

Sloshing of cryogenic liquids is a topic that has recently drawn significant attention [13][14][15][16][17][18]. This originates from the technical issues that need to be understood and controlled when designing cryogenic rocket stages (e.g. using liquid hydrogen and liquid oxygen as propellants) as well as handling long-term storage in orbit. Cryogenic propellant tanks are typically pressurized up to a certain tank pressure. In many cases this leads to the development of a thermal stratification in the liquid with saturation conditions at the free surface and a subcooled liquid bulk below. When sloshing occurs in pressurized cryogenic tanks, this might lead to the disturbance of the thermal stratification so that saturated liquid from the surface level mixes with subcooled liquid from the bulk. Thus, the surface temperature decreases and therefore the tank pressure as well, leading to condensation effects in the ullage. The reduction of the tank pressure may then lead to structural stability problems or change of the thermodynamic condition and must be compensated by in-flight helium pressurization implying to carry the sufficient amount helium.

Besides CFD simulations also experiments are conducted to better understand the occurring phenomena. In cooperation with Astrium ST the German Aerospace Center DLR in Bremen has set up a test facility which allows to test isothermal and non-isothermal (cryogenic) sloshing of liquids in various

container shapes [19]. The sloshing motion is induced by a large HexaPod (see Figure 18), which allows lateral, upward and rotational motion of the test specimen. The system is designed to carry a payload of up to 2500 kg. As shown in Figure 19, a model of the LH2 tank compartment of the A5ME upper stage is to be tested at the DLR test facility.

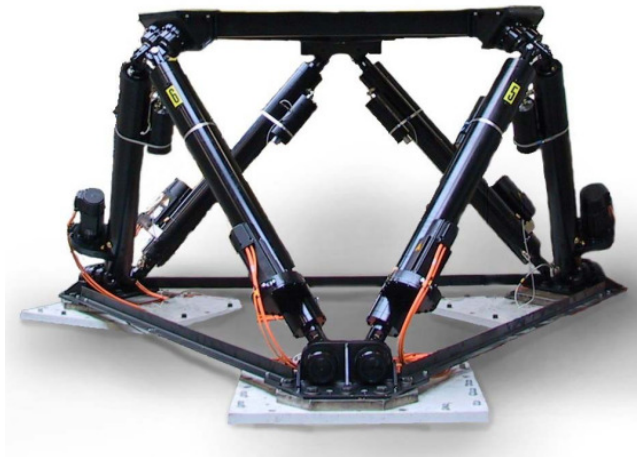


Figure 18: Image of the Bosch 6DOF HexaPod installed at DLR Bremen.

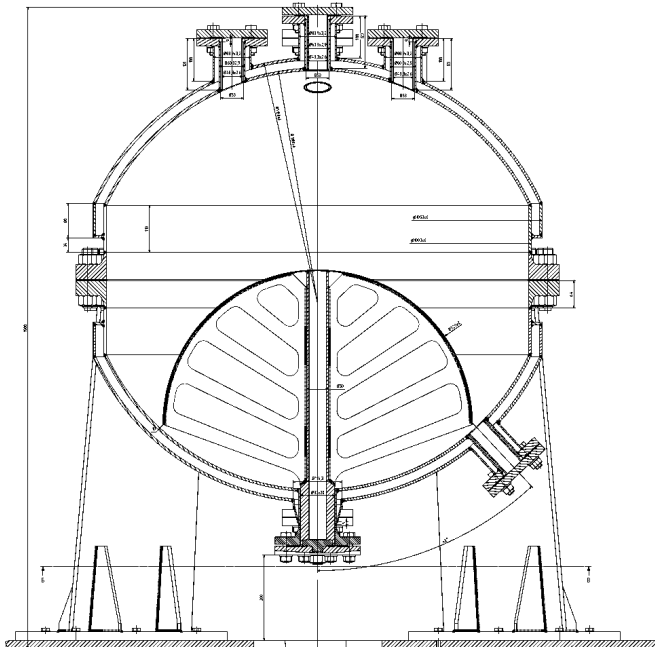


Figure 19: Drawing of the Astrium ST A5ME tank sloshing/damping demonstrator (diameter ~1 m).

9. CONCLUSION

Sloshing represents an important part of the analysis of the behaviour of liquids in propellant tanks. Not only it has to be ensured that sufficient propellant is available at the tank outlet, but also the forces and torques acting on the tank due to sloshing have to be considered for the spacecraft dynamic behaviour.

At Astrium ST a number of tools exist which are used to determine the sloshing behaviour in the propellant tanks. They may also be used to automatically generate pendulum or spring-mass models.

10. REFERENCES

- [1] J. Weiß; Smallslosh Eigenvalues and mechanical models (pendulum or spring-mass) for tanks with NEWTANK geometry; software manual and documentation; 2009
- [2] F. T. Dodge; The new "dynamic behaviour of liquids in moving containers", Southwest Research Institute; San Antonio, Texas; 2000
- [3] P. Behruzi, F. de Rose, P. Netzlaf, H. Strauch; Ballistic Phase Management for Cryogenic Upper Stages; DLRK (DGLR Conference); Bremen; 2011
- [4] P. Behruzi, H. Strauch, F. de Rose; Coasting Phase Propellant Management for Upper Stages; COSPAR Conference; Bremen; 2010
- [5] R.L. Barry and J.R. Tegart, Experimental study of transient liquid motion in orbiting spacecraft, NASA-30690, Final report, 1976
- [6] URL: www.flow3d.com
- [7] H. Klotz, R. Burkert; Coupled Flow-3D Simulation for Analysis & Modelling of Dynamics of Upper Stages Containing Liquids; 5th International Conference on Launcher Technology; Madrid, Spain; 25th-27th November 2003
- [8] D.O. Lomen; Liquid Propellant Sloshing in Mobile Tanks of Arbitrary Shape; NASA CR-R-222; 1965
- [9] H.R. Lawrence, C.J. Wang and R.B. Reddy; Variational solution of Fuel

- Sloshing Modes; Jet Propulsion, 28, pp.729-736; 1958
- [10] H.N. Abramson, W.-H. Chu and L.R. Garza; Liquid sloshing in spherical tanks; AIAA J. 1, pp. 384- 389; 1963
- [11] H.N. Abramson; Dynamic Behavior of Liquid in Moving Containers; Applied Mechanics Reviews, 16, pp. 501 - 506; 1963
- [12] H.N. Abramson; The dynamic behavior of liquids in moving containers; NASA SP-106; 1966
- [13] T. Arndt and M. Dreyer; Damping Behavior of Sloshing Liquid in Laterally Excited Cylindrical Propellant Vessels; Journal of Spacecraft and Rockets 45(5): 1085-1088; 2008
- [14] T. Arndt, M. Dreyer, P. Behruzi, M. Winter, A. van Foreest; Cryogenic Sloshing Tests in a Pressurized Cylindrical Reservoir; AIAA Joint Propulsion Conference and Exhibit, AIAA 2009-4860; Denver, Colorado; August 2009
- [15] J. Lacapere, B. Vieille and B. Legrand; Experimental and numerical results of sloshing with cryogenic fluids; EUCASS, Conference Proceeding; Brussels, Belgium; Jul. 2007
- [16] T. Himeno, Y. Umemura, S. Sugimori, S. Uzawa and T. Watanabe; Investigation on heat exchange enhanced by sloshing; AIAA Joint Propulsion Conference and Exhibit; AIAA 2009-5397; Denver, Colorado; August 2009
- [17] S.P. Das and E.J. Hopfinger; Mass transfer enhancement by gravity waves at a liquid vapor interface; Int. J. Heat Mass Tran., 52(5-6):1400-1411; 2009
- [18] M.E. Moran, N.B. McNelis, M.T. Kudlac, M.S. Habermusch and G.A. Santorino; Experimental results of hydrogen slosh in a 62 cubic foot (1750 liter) tank; AIAA Joint Propulsion Conference; AIAA-94-3259, pp. 1-10; Indianapolis, IN; June 1994
- [19] J. Gerstmann, A. van Foreest, L. Dittrich, S. Montenegro, M. Gauer, C. Manfletti, C. Hühne, R. da Costa, A. Staiger; German Research Cooperation Upper Stage; CEAS 2009 European Air and